Corrosion Science, 1975, Vol. 15, pp. 441 to 453. Pergamon Press. Printed in Great Britain

# OXIDATION STUDY OF IRON BY MÖSSBAUER CONVERSION ELECTRON AND γ-RAY SCATTERING*

A. SETTE CAMARA
Instituto de Pesquisas Radioativas, Universidade Federal de Minas Gerais, Belo Horizonte, Brazil
and
W. KEUNE
Fachbereich Angewandte Physik, Werkstoffphysik und Werkstofftechnologie, Universität des Saarlandes, 66 Saarbrücken, Germany

**Abstract**—$^{57}$Fe Mössbauer conversion electron and 14·4 keV γ-ray back-scattering have been applied to study the surface of oxidized iron samples. While γ-ray scattering explores a surface depth of about 10–20 μm, conversion electron spectra are indicative for the state of the Fe ion in the outermost surface layer up to about 3000 Å thick. Several oxide phases, like haematite, magnetite and wüstite, could be identified in the various oxide layers by their Mössbauer parameters. It is shown that the electron scattering technique is sensitive enough to allow a phase analysis and a kinetic study of oxide film growth at 500°C in an early stage, i.e. for oxidation times of the order of minutes, even if natural iron samples are used. Some examples demonstrate that due to the different depth-selectiveness of electron and γ-ray scattering spectra the combination of both techniques can give information about the type of oxide phases which are present in different surface depths.

## 1. INTRODUCTION

MÖSSBAUER experiments are usually performed by transmission geometry, i.e. the recoilless γ-rays from a source are counted after passing a resonantly absorbing thin sample.[1] Normally this method is not sensitive enough to permit surface studies since the number of Mössbauer atoms within the bulk of an absorber is usually much larger than the number of Mössbauer surface atoms, and thus surface effects usually are difficult to be detected in a transmission Mössbauer spectrum.[2] Oxidation and corrosion studies, for example of iron, performed by transmission Mössbauer spectroscopy, have often involved rather thick oxide layers or corrosion products that had been removed from the iron surfaces.[3–11]

It is also possible to observe the Mössbauer effect by detecting the radiation resonantly re-emitted by the absorber (sample). Mössbauer scattering experiments have been employed to circumvent the limitations associated with the transmission technique. The resonance scattering intensity can be monitored by means of the resonantly scattered γ-rays, the electrons resulting from the internal conversion competitive with the γ-ray emission, and characteristic X-rays and Auger electrons accompanying the conversion process. Each of these different radiations has a specific penetration range in the material the surface of which shall be investigated. Thus the surface depth reflected in the Mössbauer scattering spectrum will depend on the type of backscattered radiation which one chooses to detect, and the possibility exists to obtain Mössbauer spectra from selected regions below the surface.

Several workers have reported $^{57}$Fe Mössbauer effect measurements by re-emitted 14·4 keV γ-rays or 6·3 keV characteristic X-rays in the backscattering geometry.[12–24]

*Manuscript received 26 February 1975.

In these cases approximately 10–20 μm of sample surface depth enters into the resulting spectrum and such a deep surface layer will be more representative of the bulk of the sample rather than of its surface alone.

On the other hand, it has been shown by Swanson and Spijkerman[25] that if 7·3 keV conversion electrons and 5·4 keV Auger electrons are detected, the maximum depth of sample surface examined will be ~ 3000 Å because of the relatively small penetration range of these low-energy electrons and corresponding Mössbauer spectra will be representative of the uppermost surface layer of a sample rather than of the bulk. Recently, several investigators have demonstrated the usefulness of this technique by applying it to oxidation, corrosion and metallurgical problems.[25–34] Krakowski and Miller[35] have theoretically treated the resonance line width, resonance area and magnitude of the effect for Mössbauer conversion–electron backscattering spectra.

The present article reports $^{57}$Fe Mössbauer effect surface studies by detecting backscattering electrons and 14·4 keV γ-rays from iron samples which had been exposed to various oxidation treatments. It will be demonstrated that the Mössbauer method is sensitive enough for phase analysis and kinetic studies of surface layer growth in an early stage of oxidation even if natural iron samples (unenriched in $^{57}$Fe) are used.

## 2. EXPERIMENTAL TECHNIQUE

(a) *Detection system*

For the detection of the conversion electrons a simple gas-filled proportional counter has been built. The design is similar to the resonance counter described by Fenger[27] with a few modifications (Fig. 1). It is a flat cylindrical flow counter with an aluminized mylar entrance window for the γ-rays.

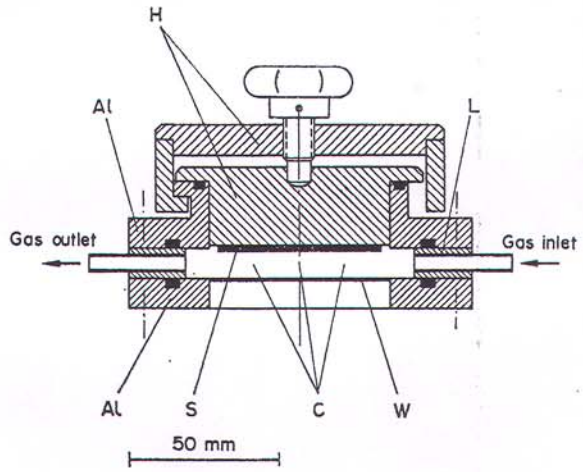


FIG. 1. Cross-section through the conversion electron gas-counter; Al—aluminium franges; L—lucite ring; W—aluminized mylar window; C—counting wires; S—sample; H—Al sample holder and bayonet catch.

The sheet-like resonance absorber (sample) which can have an outer diameter of up to 50 mm and a thickness of up to several millimetres, is placed inside of the counter. It is fixed to an Al sample holder which easily can be removed by a bayonet-catch for changing a sample. An 8 mm thick lucite ring supports three anode wires of 50 μm stainless steel wire and inlet and outlet tubes for the counting gas. Helium mixed with 2% buthane was used as a counting gas, with a flow rate of about 1 cm³/s.

The favorable operating high voltage was in the range between 750 and 900 V. Since the counter has almost no energy resolution only a lower discriminator level as a threshold for noise pulses was set, but no upper discriminator level. Measurements were performed by using a 1·5 mCi or 25 mCi source of $^{57}Co$ in a Cu matrix. A conventional electro-mechanical Mössbauer drive system operating with constant acceleration in combination with a 400- or 512-multichannel analyser operating in time mode has been used. Some of the samples have been investigated by detecting resonantly back-scattered 14·4 keV $\gamma$-rays instead of conversion electrons. For this purpose a toroidal $Ar/CH_4$ filled proportional counter was used, similar to the one described in Ref. 24.—The measuring time in all experiments was about 1–2 d for each sample.

(b) *Samples*

Polycrystalline natural iron sheets 50 mm in diameter and about 2 mm thick were used as starting material. Two kinds of samples were prepared: samples No. 1 from a carbon steel (with composition 0·04 at. %C, 0·01 %Si, 0·31 %Mn, 0·04 %P, 0·01 %S, 0·004 %Al, 0·045 %Cu) and samples No. 2 from 99·99 % pure iron. The surface to be investigated was mechanically polished and degreased, and had a shiny metallic appearance before the oxidation treatment. Various samples were prepared under several different oxidizing conditions which are characterized in Table 1. For oxidation treatments Nos. 1–3 a temperature smaller than the critical temperature for wüstite formation (570°C) was chosen,[36] while for conditions 4 and 5 the oxidation temperature was higher than this critical temperature. Oxidation under conditions 1, 2 and 4 has been performed in a closed furnace chamber which was evacuated to $10^{-4}$ Torr during the warming up of the samples from room temperature. After reaching the desired sample temperature $O_2$ atmosphere with a defined pressure was admitted to the system during a desired time period. In order to stop the oxidation the $O_2$ was pumped out rapidly and simultaneously the furnace power was switched off; subsequently the chamber was flushed rapidly with cool $N_2$ gas and the sample pulled out of the furnace. This procedure allowed to air-quench the samples to room temperature within 1–2 min. Oxidation in air (condition 3 and 5) was performed by putting the samples rapidly into a hot furnace which already had the required temperature, followed by an air quench after the desired period of oxidation.

## 3. RESULTS AND DISCUSSION

(a) *Oxidation below* 570°C

Figure 2(a) shows the 14·4 keV Mössbauer scattering spectrum of a steel sample (1) oxidized at 490°C and $10^{-3}$ Torr (condition 1, Table 1) for 1 h. A typical magnetic hyperfine split $\alpha$-iron spectrum is observed which is representative of a surface layer depth of about 10–20 $\mu$m. Obviously this technique is not sensitive enough to detect any oxide layer which has been formed during the heat treatment. The measured area ratio of the lines in Fig. 2a is 3 : 1·93 : 1·12 : 1·12 : 1·93 : 3 which is in good agreement with the theoretical area ratio of 3 : 2 : 1 : 1 : 2 : 3 which is expected in the thin absorber approximation for a statistical (random) distributions of magnetic domains[1] within the explored surface depth.

On the other hand, the conversion electron Mössbauer spectrum of a steel sample (1) which was oxidized under condition 1 for only 10 min is shown in Fig. 2(b). It is a complicated spectrum and differs remarkably from Fig. 2(a). By comparison with line

TABLE 1. THE VARIOUS OXIDATION TREATMENTS USED

| Oxidation treatment No. | Atmosphere and oxidizing temperature |
|---|---|
| 1 | $10^{-3}$ Torr $O_2$, 490°C |
| 2 | 10 Torr $O_2$, 490°C |
| 3 | air, 500°C |
| 4 | 40 Torr $O_2$, 700°C |
| 5 | air, 800°C |

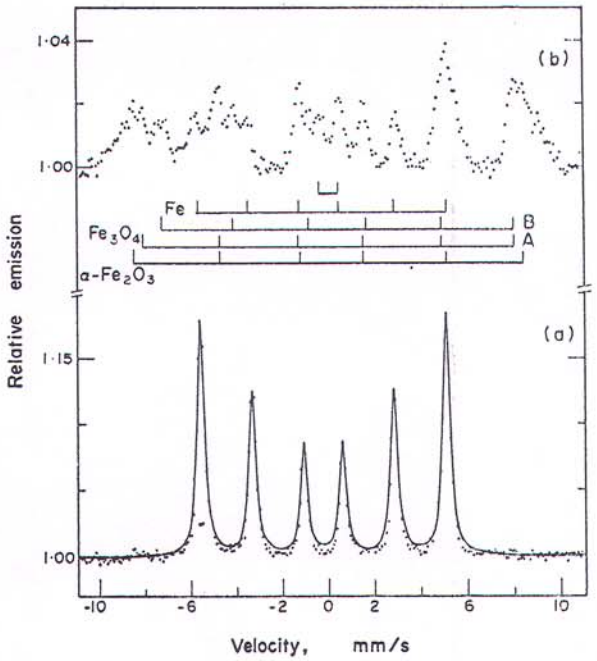


FIG. 2. (a) 14·4 keV γ-ray Mössbauer scattering spectrum from a steel sample (1) oxidized at 490°C and $10^{-3}$ Torr for 60 min;
(b) electron Mössbauer scattering spectrum from a steel sample (1) oxidized at 490°C and $10^{-3}$ Torr for 10 min (25 mCi $Co^{57}$ in Cu source).

positions of known Mössbauer spectra of bulk iron oxides[37–45] it is possible to analyse the spectrum in Fig. 2(b), which leads to the result that it is a superposition of lines due to $\alpha$-$Fe_2O_3$ and $Fe_3O_4$, the latter phase showing two magnetic hyperfine spectra corresponding to the tetrahedral *A*-sites and octahedral *B*-sites of the Fe ions. The measured hyperfine fields taken from the outer peak positions are 520 $\pm$ 8 kOe for the $\alpha$-$Fe_2O_3$ surface layer and 498 $\pm$ 8 kOe and 473 $\pm$ 8 kOe for the *A*- and *B*-sites of the $Fe_3O_4$ layer, respectively. These measured hyperfine fields agree reasonably with the corresponding values for the bulk materials, which are 517 kOe for hematite[37–39] and 491 kOe and 460 kOe for *A*- and *B*-sites of magnetite, respectively, at room temperature.[40–45] In addition to the oxide spectra the lines from the underlying $\alpha$-iron matrix are still observable in Fig. 2(b). The hyperfine patterns of the different phases are indicated as stick diagrams in the figure. (The origin of a central doublet could not be identified.) Since the lines of the $\alpha$-Fe substrate can still be observed in the electron scattering spectrum one can estimate the thickness of the total ($\alpha$-$Fe_2O_3$ plus $Fe_3O_4$) oxide surface layer (which is assumed to be continuous) to be about 2000 Å.[25] From the relative intensities of the haematite and magnetite lines one can conclude that both phases were present in the oxide layer to about equal amounts.

This phase analysis is in agreement with results by Hussey and Cohen[46] who have studied the oxidation behaviour of high purity iron (Ferrovac E) at 500°C and various $O_2$ pressures. By electron and X-ray diffraction analysis these authors could identify

an outer layer of haematite and an intermediate layer of magnetite after oxidation at $10^{-3}$ Torr and 500°C for 2 h. Thus, it was shown that at $10^{-3}$ Torr $O_2$ the $O_2$ potential is sufficiently high that $\alpha$-$Fe_2O_3$ nucleates and grows on the primarily built $Fe_3O_4$ oxide layer. In the initial stage, i.e. after oxidation for 3 min, however, only a 2800Å thick layer of magnetite has been identified by electron and X-ray analysis.[46] The present result (Fig. 2b) shows that for steel sample 1 investigated here the $\alpha$-$Fe_2O_3$ formation at 490°C and $10^{-3}$ Torr sets in already in an early stage, i.e. after a time of oxidation of 10 min or smaller.

The 14·4 keV $\gamma$-ray Mössbauer spectra of steel samples (1) which were oxidized at 10 Torr $O_2$ and 490°C (condition 2, Table 1) for 10 and 30 min are shown in Fig. 3(a) and (b), respectively. In addition to the dominant $\alpha$-Fe pattern of the underlying substrate weaker magnetite lines can be seen. The measured line intensity ratios for the hyperfine patterns are about 3 : 2 : 1 : 1 : 2 : 3 which is characteristic for a random spin arrangement within the explored sample depth (10–20 $\mu$m). The hyperfine fields agree with corresponding bulk values. The relative intensity of the $Fe_3O_4$ lines increases with longer oxidation time (from 16 area % in Fig. 3a to 24

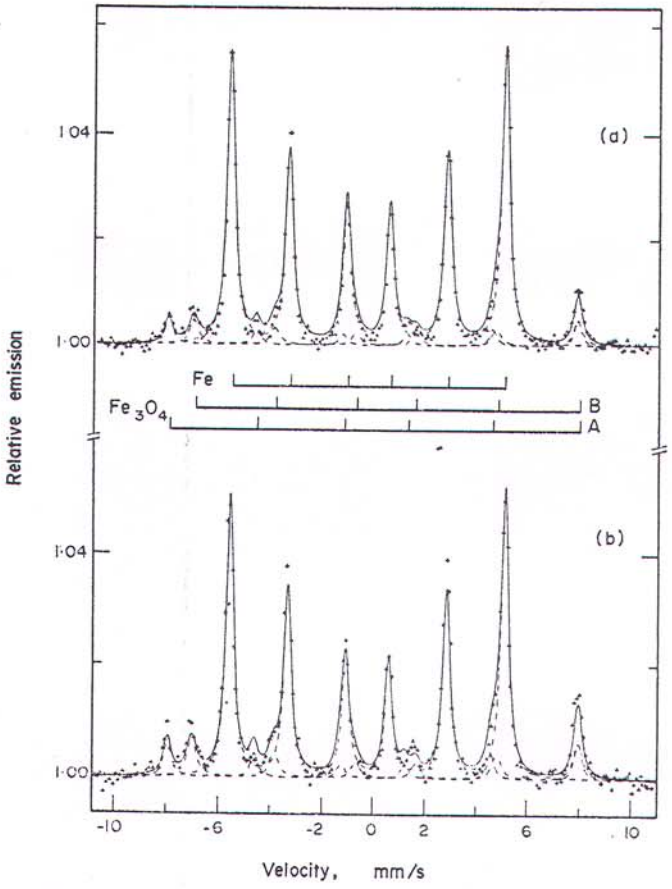


FIG. 3. 14·4 keV $\gamma$-ray scattering spectra from steel samples (1) oxidized at 490°C and 10 Torr $O_2$ for (a) 10 min, and (b) 30 min (25 mCi $Co^{57}$ in Cu source).

area % in Fig. 3b). From this relative intensity a $Fe_3O_4$ film thickness of the order of a few $10^4$ Å can be roughly estimated.

For the intensity ratio (area ratio) of the *B*-site spectrum to the *A*-site spectrum in Fig. 3(a or b) a value of $1{\cdot}3 \pm 0{\cdot}3$ has been obtained which deviates from the expected intensity ratio of 2·0 for stoichiometric magnetite. Furthermore, a line broadening of the outer lines of the *B*-site spectrum of 20% as compared to the outer lines of the *A*-site pattern has been measured. Similar observations have been made with non-stoichiometric magnetite[43–45] and ascribed to the effect of cation vacancies on *B*-sites. Thus, we conclude that the magnetite layer of the steel samples oxidized under condition 2 were non-stoichiometric, with an estimated vacancy concentration of about 4% or larger.[43–45]

Comparison of Fig. 3(a, b) with Fig. 2(a) shows clearly that (at least for oxidation times smaller than 1 h) the oxide formation at 490°C depends strongly on the oxygen pressure, i.e. the amount of oxide increases with increasing $O_2$ pressure at equal times of oxidation. In this respect the behaviour of the steel sample (1) is different from that of high purity iron. For the latter material (Ferrovac E) the oxidation kinetics in the $O_2$ pressure range of $10^{-3}$–75 Torr at 450–500°C has been found to be essentially independent of pressure after oxidation times of up to 3 h.[46] On the other hand, our steel samples 1 showed already a relatively thick $Fe_3O_4$ layer after only 10 min and 30 min of oxidation at 10 Torr (Fig. 3), while such a thick oxide layer could not be detected at $10^{-3}$ Torr even after 60 min of oxidation (Fig. 2a). Furthermore, it is remarkable that no haematite lines can be observed in the spectra of Fig. 3. This indicates that an outer $\alpha$-$Fe_2O_3$ layer, which is expected to be present at 10 Torr $O_2$ and 490°C,[46] is too thin to be detectable by $\gamma$-ray scattering, and hence must have a thickness of the order of several 1000 Å only. This is in contrast to the oxide film composition found for high purity iron for which already after 3 min of oxidation at 10 Torr and 500°C $\alpha$-$Fe_2O_3$ is present to about the same extent as $Fe_3O_4$, and with increasing time of oxidation $\alpha$-$Fe_2O_3$ becomes the major constituent.[46]

A kinetic study of oxide layer growth has been performed on several pure Fe samples (No. 2) which were oxidized in air at 500°C (condition 3, Table 1). Mössbauer electron scattering spectra of these samples oxidized under condition 3 for 0, 45, 90, 180 and 300 s are shown in Fig. 4. The spectra are characterized by a gradual change from an initially pure $\alpha$-Fe hyperfine pattern (top) to a superposition of $\alpha$-Fe, $Fe_3O_4$ and $\alpha$-$Fe_2O_3$ spectra with increasing oxidation time, until finally (oxidized for 300 s) only a pure $\alpha$-$Fe_2O_3$ spectrum is observed. The pure $\alpha$-Fe spectrum has a line intensity ratio (area ratio) of 3 : 3·63 : 1·17 : 1·17 : 3·63 : 3 which is close to the ratio 3 : 4 : 1 : 1 : 4 : 3 which one expects for an angle of 90° between the incident $\gamma$-ray direction and the magnetization (or spin) direction.[1] Thus, the magnetization within a surface depth of $\sim$ 3000 Å in $\alpha$-Fe lies preferentially parallel to the surface. This result should be compared with the 14·4 keV scattering spectrum of $\alpha$-Fe in Fig. 2(a) which shows that averaged over a layer depth of $\sim$ 100,000 Å the magnetization is randomly distributed.

The measured hyperfine fields for the $Fe_3O_4$ layers (Fig. 4) are $496 \pm 8$ kOe and $467 \pm 5$ kOe for *A*- and *B*-sites, respectively and agree within error limits with corresponding values for bulk magnetite. For the $\alpha$-$Fe_2O_3$ layers the hyperfine field is $518 \pm 5$ kOe, and the quadrupole interaction constant is $e^2qQ/2 = 0{\cdot}40 \pm 0{\cdot}10$ mm/s, also in agreement with bulk values.[37–39] An important fact concerning the correlation

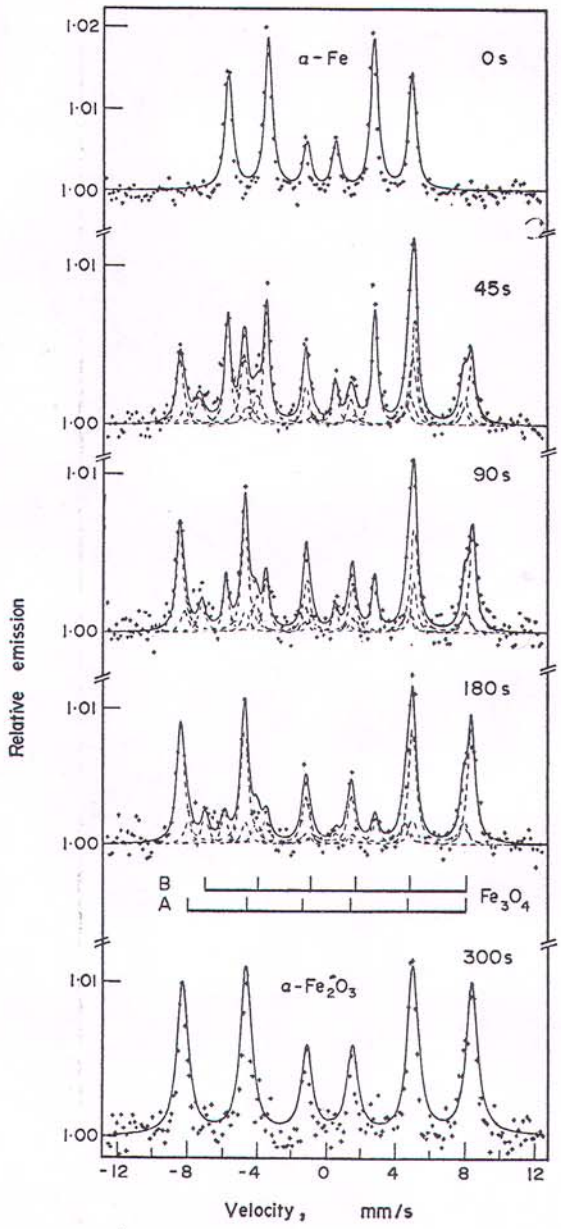


FIG. 4. Electron Mössbauer scattering spectra from pure iron samples (2) oxidized at 500°C in air for 0, 45, 90, 180 and 300 s (1·5 mCi $Co^{57}$ in Cu source).

of oxide layer growth with the underlying substrate can be observed in the pure $\alpha$-$Fe_2O_3$ spectrum (Fig. 4, bottom). This spectrum has a measured line intensity ratio (area ratio) of 3 : 3·1 : 1·2 : 1·2 : 1 : 3 which deviates remarkably from the intensity ratio of 3 : 2 : 1 : 1 : 2 : 3 for a polycrystalline surface layer with a random spin

distribution. This indicates a tendency for the spins in the antiferromagnetic $\alpha$-$Fe_2O_3$ surface layer ($\sim$ 3000 Å thick) to be aligned preferentially parallel to the surface, as in the ferromagnetic $\alpha$-iron substrate. Since the spin direction of antiferromagnetic $\alpha$-$Fe_2O_3$ at room temperature is perpendicular to the crystallographic $c$-axis[47-49] one can conclude that the growth of these haematite layers at 500°C in air occurred with the $c$-axis preferentially oriented perpendicular to the oxide–metal interface. A crystallographic texture in $\alpha$-$Fe_2O_3$ and $Fe_3O_4$ oxide layers of polycrystalline iron has been observed also by Boggs *et al.*[50] by electron diffraction.

For the $Fe_3O_4$ phase a computer fit of the spectra in Fig. 4 resulted in an integrated line intensity ratio of about 3 : 3 : 1 : 1 : 3 : 3 for both $A$- and $B$-sites, which indicates that also for this phase the magnetization was preferentially oriented parallel to the surface plane. No definite conclusion about the population of $A$- and $B$-sites in the $Fe_3O_4$ layer could be drawn, since the measured area ratio of the $B$-site to the $A$-site hyperfine patterns was 1·5 $\pm$ 0·5 as compared to a ratio of 2·0 for stoichiometric bulk magnetite, and the uncertainty in the former value is too large. In Table 2 the measured relative area (%) of the hyperfine patterns caused by the oxide layer ($\alpha$-$Fe_2O_3$ plus $Fe_3O_4$) as compared to the total measured area (100%) in each spectrum of Fig. 4 is given for the various oxidation times.

In kinetic studies the laws of oxide layer growth as a function of oxidation time are usually given for the absolute oxide layer thickness (in cm). Thus the area-percent oxide thickness determined from the Mössbauer spectra has to be converted to its corresponding absolute oxide layer thickness $d$. This has been done in the following approximate way. Swanson and Spijkerman[25] have measured the relative areas in Mössbauer conversion electron scattering spectra of thin iron films of known thickness evaporated on to thick stainless steel substrates. They obtained values of 65 area % for a 600 Å Fe film, and 96 area % for a 3000 Å thick Fe film, relative to the total area (100%) under the Mössbauer spectra. We have used these calibration points and the origin (0% effect for $d = 0$) and interpolated between them by fitting a $d^{1/4}$ dependence for the relative area vs $d$ relation. The absolute oxide layer thickness $d$ corresponding to each relative area in Table 2 (and for the relative area of some additional samples) was then approximately determined by using this relation. A plot of the total oxide layer thickness $d$ ($Fe_3O_4$ plus $\alpha$-$Fe_2O_3$) obtained in this way vs the square-root of oxidation time, $t^{1/2}$, results in Fig. 5. A straight line* can be fitted to the

TABLE 2. RELATIVE AREA (%) OF OXIDE LAYER ($Fe_3O_4$ PLUS $x$-$Fe_2O_3$) AS A FUNCTION OF OXIDATION TIME $t$ ACCORDING TO FIG. 4

| Oxidation time $t$ (s) | Relative area of oxide layer % |
|---|---|
| 0 | 0 |
| 45 | 59·6 |
| 90 | 78·1 |
| 180 | 88·5 |
| 300 | 100 |

*The straight line in Fig. 5 does not pass through the $d$–$t^{1/2}$–origin; the reason is that the given oxidation times include the warm-up time from room-temperature to 500°C (equal for all samples) during which the oxidation proceeds more slowly.

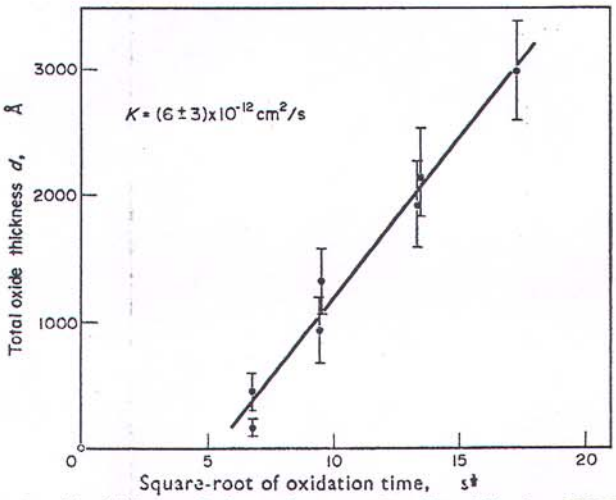


FIG. 5. Total oxide thickness $d$ of pure iron samples (2) oxidized at 500°C in air as a function of the square-root of oxidation time, $t^{1/2}$.

data points the slope of which yields a value for the parabolic oxidation rate constant $K$ of $(6 \pm 3) \times 10^{-12}$ cm²/sec. Our value for $K$ can be compared with the parabolic rate constant of high purity iron at 500°C which one can calculate from listed $d$ values given by Hussey and Cohen[46] for the initial stage of oxide layer growth. These given values are $d = 2800$ Å at $10^{-3}$ Torr and $d = 2500$ Å at 10 Torr $O_2$ pressure for 3 min oxidation time, the rate being fairly independent of $O_2$ partial pressure at the initial growth stage. This leads to $K$ values of $4{\cdot}4 \times 10^{-12}$ cm²/s and $3{\cdot}5 \times 10^{-12}$ cm²/s, respectively. Thus, our above oxidation rate constant is in satisfactory agreement with these values.

(b) *Oxidation above* 570°C

The common dominant feature in the 14·4 keV γ-ray Mössbauer scattering spectra of two steel samples (1) which were oxidized at 700°C and 40 Torr $O_2$ (condition 4, Table 1) for 10 min and 30 min (Fig. 6(a) and (b), respectively) is an intense, partially resolved doublet which exhibits a definite asymmetry in the two peak heights. The position of these peaks (with respect to α-Fe) are at $+ 0{\cdot}75 \pm 0{\cdot}04$ and $1{\cdot}18 \pm 0{\cdot}03$ mm/s in Fig. 6(a) and at $+ 0{\cdot}65 \pm 0{\cdot}03$ and $+ 1{\cdot}22 \pm 0{\cdot}02$ mm/s in Fig. 6(b). These doublet spectra are in agreement with Mössbauer absorption measurements in divalent iron oxide, i.e. wüstite ($Fe_{1-x}O$), by several authors[51–57] who have shown that the two peaks with unequal intensity are caused by a superposition of quadrupole split $Fe^{2+}$ lines and a $Fe^{3+}$ single line arising as a result of the defect structure with cation vacancies in this compound with NaCl structure. The separation of the two peaks diminishes from about 0·7 mm/s for $x \lesssim 0{\cdot}083$[57] to 0·00 mm/s for (metastable) stoichiometric $Fe_{1{\cdot}0}$.[58] From the measured peak separation of the wüstite lines in Fig. 6(a and b) we can roughly estimate an upper limit for the average composition $x$ of our wüstite surface layers of $x \gtrsim 0{\cdot}05$. Since the doublet is not as well resolved in Fig. 6(a) as in Fig. 6(b) the sample oxidized for 10 min must have an average composition closer to stoichiometry than the 30 min sample.

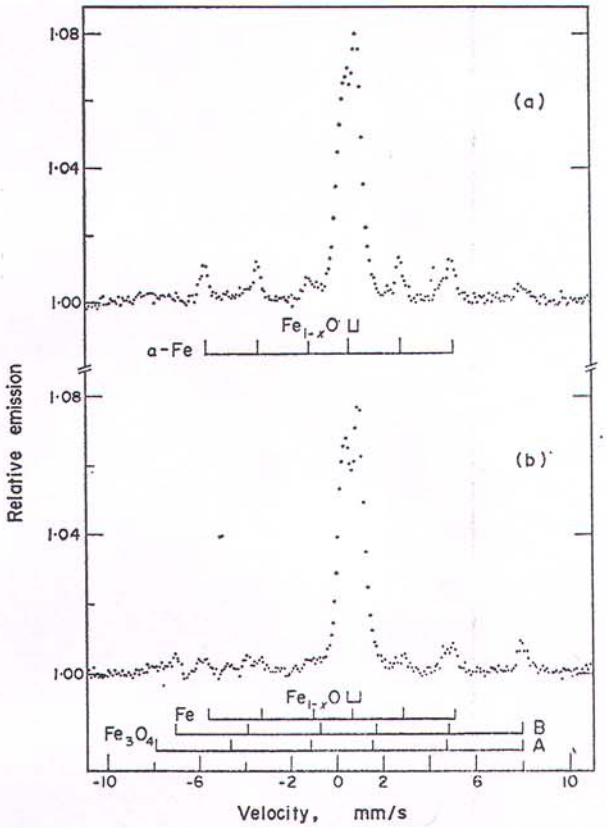


FIG. 6. 14·4 keV γ-ray scattering spectrum of steel samples (1) oxidized at 700°C and 40 Torr $O_2$ for (a) 10 min and (b) 30 min (25 mCi $Co^{57}$ in Cu source).

In addition to the strong wüstite lines a weaker α-Fe pattern caused by the underlying substrate can be observed in Fig. 6(a) and with less intensity in Fig. 6(b). This implies a wüstite thickness of roughly 10 μm. Also additional magnetite lines clearly appear in Fig. 6(b) and with weaker intensity in Fig. 6(a). The observation of the $Fe_3O_4$ phase is in agreement with the conception that the oxide layer consists in two parts, namely an inner wüstite layer and an outer $Fe_3O_4$ layer in equilibrium with each other.[59] The thickness of the $Fe_3O_4$ layer can be estimated from Fig. 6 to be roughly 10–20% of the wüstite layer. However, we cannot exclude entirely the possibility that a small fraction of the magnetite observed in Fig. 6 was formed by precipitation in the metastable wüstite matrix.[60,61] No haematite lines could be identified in Fig. 6. Thus an outer haematite overgrowth on top of the $Fe_3O_4$ layer[62] was too thin (several 1000 Å only) to be detectable by γ-ray scattering.

On the other hand, haematite could be identified by Mössbauer electron scattering spectra of two pure iron samples (2) oxidized at 800°C in air (condition 5, Table 1) for 16 and 60 s (Fig. 7 a and b, respectively). Predominantly α-$Fe_2O_3$ lines and weaker $Fe_3O_4$ lines can be observed in both spectra, but a wüstite line cannot be identified with certainty. We conclude that the first few 1000 Å of the oxide film consisted in an

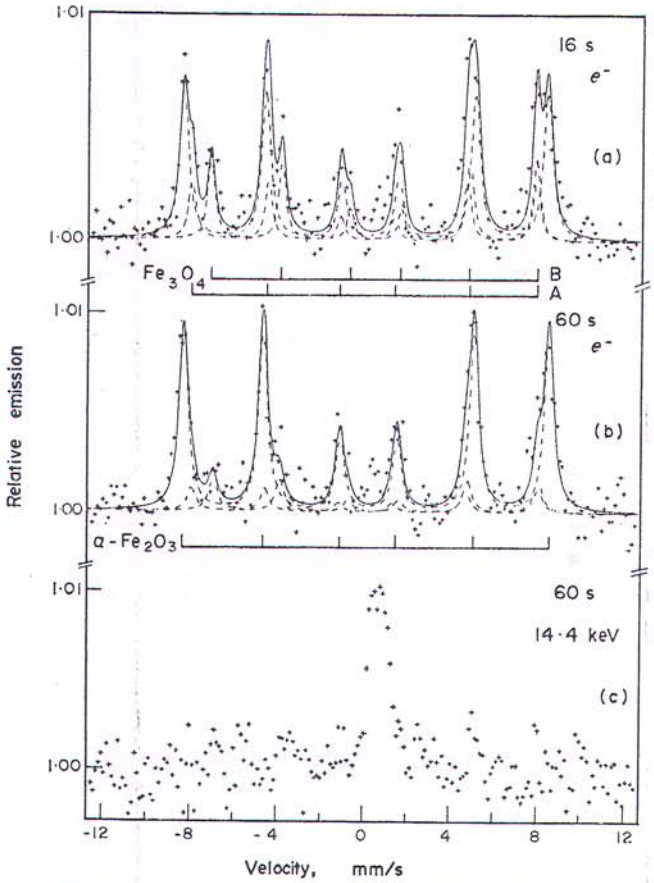


FIG. 7. Electron Mössbauer scattering spectra of iron samples (2) oxidized at 800°C in air for (a) 16 s and (b) 60 s; (c) 14·4 keV γ-ray scattering spectrum of the same sample as in (b) (1·5 mCi $Co^{57}$ in Cu source).

outer $\alpha$-$Fe_2O_3$ layer followed by $Fe_3O_4$. With increasing oxidation time the $Fe_3O_4$ intensity decreases relative to that of the haematite which means that the $\alpha$-$Fe_2O_3$ layer thickness increases with longer oxidation. The same sample as in Fig. 7(b) has been investigated also by γ-ray scattering. Within the statistical error the obtained spectrum (Fig. 7c) indicated only the presence of the wüstite phase. Thus, we can conclude that the oxide film after 60 s of oxidation was composed of a $\sim$ 2000 Å thick surface layer of $\alpha$-$Fe_2O_3$ and of an intermediate layer of $Fe_3O_4$, which was followed by a thick ($\sim$ 10–20 μm) layer of wüstite. This result agrees well with the phase analysis performed by other measuring techniques on iron samples oxidized at 800°C.[62]

## 4. CONCLUSION

In the present investigation the usefulness of $^{57}Fe$ Mössbauer conversion electron and 14·4 keV γ-ray backscattering for the phase analysis of iron oxide layers *in situ* was demonstrated by several examples. While γ-ray scattering explores a surface

depth of 10–20 μm, conversion electron spectra are indicative for the state of the Fe ion in the outermost surface layer up to about 3000 Å thick. The spectra showed that oxidation of iron near 500°C at various $O_2$ partial pressures resulted in layers of $\alpha$-$Fe_2O_3$ and $Fe_3O_4$. Analysis of the relative line intensities of the different phases in the spectra leads to the result that the kinetics of oxide layer growth of pure iron at 500°C in air in an early stage (i.e. between about 1–5 min of oxidation) follows most likely a parabolic law, with a measured rate constant of $K = (6 \pm 3) \times 10^{-12}$ cm²/s. Mössbauer line intensity ratios indicated that under these latter oxidizing conditions the growth of $\alpha$-$Fe_2O_3$ on polycrystalline pure iron occurs with a pronounced crystallographic texture. In samples prepared at higher temperatures (700–800°C) non-stoichiometric wüstite, $Fe_{1-x}O$, has been found to be the main component in the oxide layers, but in addition a relatively thin outer layer of haematite and an intermediate layer of magnetite could be identified by conversion electron scattering.

*Acknowledgements*—The authors are grateful to Dr. R. Thiele for providing the oxidized steel samples, and for helpful discussions with him and with Dr. U. Gonser. This work was supported in part by the International Atomic Energy Agency, Vienna, by the Institut de Recherches de la Sidérurgie Francaise (IRSID) and by the Deutsche Forschungsgemeinschaft.

## REFERENCES

1. See, for example: *Chemical Applications of Mössbauer Spectroscopy*, edited by V. I. GOLDANSKII and R. H. HERBER. Academic Press, New York, 1968; N. N. GREENWOOD and T. C. GIBB, *Mössbauer Spectroscopy*. Chapman and Hall, London (1971).
2. V. I. GOLDANSKII and I. P. SUZDALEV, in: Proc. Intern. Conf. on Applications of the Mössbauer Effect, Tihany, Hungary, edited by I. DÉZSI, p. 269. Akadémiai Kiadó, Budapest (1971).
3. I. DÉZSI, A. VERTES and L. KISS, *J. Radioanal. Chem.* **2**, 183 (1964).
4. D. D. JOYE and R. C. AXTMANN, *Anal. Chem.* **40**, 876 (1968).
5. L. J. SWARTZENDRUBER and L. H. BENNETT, *Scripta Met.* **2**, 93 (1968).
6. A. M. PRITCHARD and C. M. DOBSON, *Nature* **224**, 1295 (1969).
7. D. A. CHANNING and M. J. GRAHAM, *J. electrochem. Soc.* **117**, 389 (1970).
8. G. M. BANCROFT, J. E. O. MAYNE and P. RIDGEWAY, *Brit. Corros. J.* **6**, 119 (1971).
9. A. M. PRITCHARD, J. R. HADDON and G. N. WALTON, *Corros. Sci.* **11**, 11 (1971).
10. A. M. PRITCHARD and B. T. MOULD, *Corros. Sci.* **11**, 1 (1971).
11. D. A. CHANNING and M. J. GRAHAM, *Corros. Sci.* **12**, 271 (1972).
12. J. K. MAJOR, in: *Mössbauer Effect Methodology*, Vol. 1, edited by I. J. GRUVERMAN, p. 89. Plenum Press, New York (1965).
13. P. DEBRUNNER, in: *Mössbauer Effect Methodology*, Vol. 1, edited by I. J. GRUVERMAN, p. 97. Plenum Press, New York (1965).
14. R. C. KOCH, H. K. CHOW and R. L. BOGNER, Mössbauer Spectrometry for Analysis of Iron Compounds, U.S. Atomic Energy Commission Report No. NSEC-4010-1 (1967).
15. R. H. FORSYTH and J. H. TERREL, *Bull. Am. Phys. Soc.* **13**, 61 (1968).
16. J. H. TERREL and J. J. SPIJKERMAN, *J. appl. Phys.* **13**, 11 (1968).
17. R. L. COLLINS, in: *Mössbauer Effect Methodology*, Vol. 4, edited by I. J. GRUVERMAN, p. 129. Plenum Press, New York (1968).
18. R. N. ORD, *Appl. Phys. Lett.* **15**, 279 (1969); R. N. ORD, Mössbauer effect using backscatter geometry as applied to non-destructive testing, U.S. Atomic Energy Commission Report No. BNWL-1276 (1969).
19. H. K. CHOW, R. F. WEISE and P. A. FLINN, Mössbauer Spectrometry for Analysis of Iron Compounds, U.S. Atomic Energy Commission Report No. NSEC-4023-1 (1969).
20. H. A. STÖCKLER, *J. appl. Phys.* **41**, 825 (1970).
21. W. MEISEL, *Werkstoffe und Korrosion* **21**, 249 (1970).
22. P. OSTERGAARD, *Nucl. Instrum. Meth.* **77**, 328 (1970).
23. R. N. ORD and C. L. CHRISTENSEN, *Nucl. Instrum. Meth.* **91**, 293 (1971).
24. B. KEISCH, *Nucl. Instrum. Meth.* **104**, 237 (1972).
25. K. R. SWANSON and J. J. SPIJKERMAN, *J. appl. Phys.* **41**, 3155 (1970).
26. ZW. BONCHEV, A JORDANOV and A. MINKOVA, in: *Proc. Intern. Conf. on Application of the Mössbauer Effect*, Tihany, Hungary, edited by I. DZÉSI. Akadémiai Kiadó, Budapest (1971).

27. J. FENGER, *Nucl. Instrum. Meth.* **69**, 268 (1969); **106**, 203 (1973).
28. H. ONODERA, H. YAMAMOTO, H. WATANABE and H. EBIKO, *Jap. J. appl. Phys.* **11**, 1380 (1972).
29. L. J. SWARTZENDRUBER and L. H. BENNETT, *Scripta Met.* **6**, 737 (1972).
30. R. L. COLLINS, R. A. MAZAK and C. M. YAGNIK, in: *Mössbauer Effect Methodology*, Vol. 8, edited by I. J. GRUVERMAN, p. 191. Plenum Press, New York (1973).
31. V. STEFÁNSSON and D. LILJEQUIST, *Nucl. Instrum. Meth.* **115**, 373 (1974).
32. T. EKDAHL, B. RINGSTRÖM and U. BÄVERSTAM, University of Stockholm, Institute of Physics Report No. USIP-74-14 (1974).
33. G. W. SIMMONS, E. KELLERMAN and H. LEIDHEISER, JR., *Corrosion-NACE* **29**, 227 (1973).
34. C. M. YAGNIK, R. A. MAZAK and R. L. COLLINS, *Nucl. Instrum. Meth.* **114**, 1 (1974).
35. R. A. KRAKOWSKI and R. B. MILLER, *Nucl. Instrum. Meth.* **100**, 93 (1972).
36. M. HANSEN and K. ANDERKO, *Constitution of Binary Alloys*, p. 684. McGraw-Hill, New York (1958).
37. O. C. KISTNER and A. W. SUNYAR, *Phys. Rev. Lett.* **4**, 412 (1960).
38. K. ONO and A. ITO, *J. Phys. Soc. Japan* **17**, 1012 (1962).
39. F. VAN DER WOUDE, *Phys. Stat. Sol.* **17**, 417 (1966).
40. R. BAUMINGER, S. G. COHEN, A. MARINOV, S. OFER and E. SEGAL, *Phys. Rev.* **122**, 1447 (1961).
41. A. ITO, K. ONO and Y. ISHIKAWA, *J. Phys. Soc. Japan* **18**, 1465 (1963).
42. F. VAN DER WOUDE, G. A. SAWATZKY and A. H. MORRISH, *Phys. Rev.* **167**, 533 (1968).
43. J. M. DANIELS and A. ROSENCWAIG, *J. Phys. Chem. Solids* **30**, 1561 (1969).
44. B. J. EVANS and S. S. HAFNER, *J. appl. Phys.* **40**, 1411 (1969).
45. V. P. ROMANOV and V. D. CHECHERSKII, *Fizika Tverdogo Tela* **12**, 1853 (1970); *Soviet Phys.—Solid State* **12**, 1474 (1970).
46. R. J. HUSSEY and M. COHEN, *Corros. Sci.* **11**, 713 (1971).
47. F. J. MORIN, *Phys. Rev.* **78**, 819 (1950).
48. C. G. SHULL, W. A. STRAUSER and E. D. WOLLAN, *Phys. Rev.* **83**, 333 (1951).
49. J. A. EATON and A. H. MORRISH, *J. appl. Phys.* **40**, 3180 (1969).
50. W. E. BOGGS, R. H. KACHIK and G. E. PELLISSIER, *J. electrochem. Soc.* **112**, 539 (1965).
51. G. K. WERTHEIM, *J. appl. Phys.* **32**, 110 S (1961).
52. G. SHIRANE, D. E. COX and S. L. RUBY, *Phys. Rev.* **125**, 1158 (1962).
53. H. SHECHTER, P. HILLMAN and M. RON, *J. appl. Phys.* **37**, 3043 (1966).
54. R. W. VAUGHAN and H. G. DRICKAMER, *J. Chem. Phys.* **47**, 1530 (1967).
55. D. P. JOHNSON, *Solid St. Commun.* **7**, 1785 (1969).
56. H. U. HRYNKIEWICZ, D. S. KULGAWCZUK, E. S. MAZANEK, A. M. PUSTOWKA, K. TOMALA and M. E. WYDERKO, *Phys. status solidi* (a) **9**, 611 (1972).
57. V. P. ROMANOV, L. F. CHECHERSKAYA and P. A. TATSIENKO, *Phys. status solidi* (a) **15**, 721 (1973).
58. B. HENTSCHEL, *Z. Naturforschung* **25a**, 1996 (1970).
59. M. DAVIES, M. SIMNAD and C. BIRCHENALL, *J. Metals* **3**, 889 (1951).
60. A. HOFFMANN, *Z. Elektrochemie* **63**, 207 (1959).
61. B. ILSCHNER and E. MLITZKE, *Acta Met.* **13**, 855 (1965).
62. A. G. GOURSAT and W. W. SMELTZER, *Oxidation of Metals* **6**, 101 (1973).